Flow cytometry analysis reveals a decrease in intracellular sodium during sperm capacitation

Jessica Escoffier[1], Dario Krapf[2], Felipe Navarrete[1], Alberto Darszon[3,*] and Pablo E. Visconti[1,*]

[1]Department of Veterinary and Animal Science, Integrated Sciences Building, University of Massachusetts, Amherst, MA, USA
[2]Institute of Molecular and Cell Biology of Rosario (CONICET-UNR), Argentina
[3]Department of Developmental Genetics and Molecular Physiology, IBT-UNAM, Cuernavaca, México
*Authors for correspondence (darszon@ibt.unam.mx; anpvisconti@vasci.umass.edu)

Accepted 12 September 2011
Journal of Cell Science 125, 473–485

doi: 10.1242/jcs.093344

Summary

Mammalian sperm require time in the female tract in order to be able to fertilize an egg. The physiological changes that render the sperm able to fertilize are known as capacitation. Capacitation is associated with an increase in intracellular pH, an increase in intracellular calcium and phosphorylation of different proteins. This process is also accompanied by the hyperpolarization of the sperm plasma membrane potential. Recently, we presented evidence showing that epithelial Na^+ channels (ENaC) are present in mature sperm and that ENaCs are blocked during capacitation. In the present work, we used flow cytometry to analyze changes in intracellular Na^+ concentration ($[Na^+]_i$) during capacitation in individual cells. Our results indicate that capacitated sperm have lower Na^+ concentrations. Using sperm with green fluorescent protein in their acrosomes, it was shown that the lower $[Na^+]_i$ concentration only occurs in sperm having intact acrosomes. ENaC inhibition has been shown in other cell types to depend on the activation of cystic fibrosis transmembrane conductance regulator (CFTR). In non-capacitated sperm, amiloride, an ENaC inhibitor, and genistein, a CFTR activator, caused a decrease in $[Na^+]_i$, suggesting that also in these cells $[Na^+]_i$ is dependent on the crosstalk between ENaC and CFTR. In addition, PKA inhibition blocked $[Na^+]_i$ decrease in capacitated sperm. Altogether, these data are consistent with the hypothesis that the capacitation-associated hyperpolarization involves a decrease in $[Na^+]_i$ mediated by inhibition of ENaC and regulated by PKA through activation of CFTR channels.

Key words: Capacitation, Flow cytometry, ENaC, CFTR, Hyperpolarization, Membrane potential, Sodium

Introduction

After ejaculation, sperm are still unable to fertilize. They gain their fertilizing ability in the female genital tract (Yanagimachi, 1994). The physiological and molecular events that render the sperm able to fertilize are collectively known as capacitation. Although this process was discovered 60 years ago (Austin, 1952; Chang, 1951), the molecular mechanisms of sperm capacitation are still poorly understood. In mouse sperm, capacitation depends on lipid remodeling of the plasma membrane (Trevino et al., 2001; Visconti et al., 1999a; Visconti et al., 1999b), increase of intracellular pH (Nakanishi et al., 2001; Zeng et al., 1996), increase in protein tyrosine phosphorylation (Arcelay et al., 2008; Krapf et al., 2010; Visconti et al., 1995a; Visconti et al., 1995b) and changes in fluxes of ions such as Ca^{2+}, HCO_3^-, K^+ and Na^+ (Arnoult et al., 1997; Demarco et al., 2003; Felix et al., 2002; Munoz-Garay et al., 2001). These events are associated with functional sperm parameters such as hyperactivated motility (Yanagimachi, 1994), the ability to undergo a physiological stimulated acrosome reaction (Buffone et al., 2008; Escoffier et al., 2010b; Tomes, 2007) and the ability to penetrate the egg.

Among ion fluxes occurring during capacitation, transport of HCO_3^- (Demarco et al., 2003) constitutes one essential step in the initiation of capacitation. Influx of HCO_3^- into sperm promotes cAMP synthesis through activation of the atypical soluble adenylyl cyclase (Esposito et al., 2004; Hess et al., 2005) and subsequent protein kinase A (PKA) activation. This activation of a cAMP-dependent pathway is upstream of the capacitation-associated increase in tyrosine phosphorylation (Visconti, 2009). It has been shown that capacitation in mouse sperm is also accompanied by hyperpolarization of the sperm plasma membrane potential (E_m) (Arnoult et al., 1999). The molecular mechanism of this hyperpolarization is not clear. Previous studies by our group indicate that Na^+ permeability is involved in the establishment of the sperm resting E_m and that this Na^+ permeability is reduced during sperm capacitation (Demarco et al., 2003; Hernandez-Gonzalez et al., 2006). These results are consistent with the hypothesis that electrogenic Na^+ transport is reduced during sperm capacitation, resulting in hyperpolarization. In this work, it is shown that in a Na^+-free medium, addition of Na^+ induced a fast depolarization of the sperm E_m. Interestingly, this depolarization was blocked by both amiloride and 5-(*N*-ethyl-*N*-isopropyl) amiloride (EIPA), an amiloride analogue, suggesting that epithelial Na^+ channels (ENaCs) were involved in this Na^+ permeability. ENaCs are made up of four subunits: α, β, γ and δ, where α and δ can replace each other and are directly involved in forming the channel pore (Canessa et al., 1994). Using antibodies against ENaC subunits, we had previously demonstrated the presence of ENaC-α and ENaC-δ in mouse sperm (Hernandez-Gonzalez et al., 2006). By contrast, patch-clamp current recordings in testicular sperm detected an amiloride-sensitive component consistent with the presence of ENaCs in these cells (Martinez-Lopez et al., 2009).

However, how the ENaC is regulated during sperm capacitation is not known. In other cell types, it has been shown that cystic fibrosis transmembrane conductance regulator (CFTR) inactivates ENaC, either through direct stimulation involving the first nucleotide binding domain of CFTR (Schreiber et al., 1999) or through increase of intracellular Cl^- concentration (Konig et al., 2001). More recently, work by our group as well as others have demonstrated the presence of this Cl^- channel in mammalian sperm (Hernandez-Gonzalez et al., 2007), opening the possibility of a similar regulatory pathway in these cells.

Regarding signaling pathways associated with sperm capacitation, it is necessary to consider that only a fraction of the sperm population undergoes capacitation. Owing to difficulties in experimental conditions, most studies on the molecular basis of capacitation have been done with complete sperm suspensions containing sperm in different stages of capacitation, as well as subpopulations of deteriorated sperm cells. To solve problems related to sperm heterogeneity and compartmentalization during capacitation, recent studies have used flow cytometry (Martinez-Pastor et al., 2010; Nakanishi et al., 2001; Piehler et al., 2006; Tao et al., 1993), single cell analysis (Arnoult et al., 1999; Escoffier et al., 2007; Fukami et al., 2003) and combinations of both, that is, microscopy visualization of signaling pathways after sorting of sperm subpopulations by flow cytometry (de Vries et al., 2003; Flesch et al., 2001). Altogether, these experimental approaches are vital for understanding how sperm capacitation occurs and to discriminate certain features between live and degenerating sperm that can skew the conclusions of a particular experiment.

In this work, we used flow cytometry to qualitatively analyze changes in intracellular Na^+ concentration ($[Na^+]_i$). For this purpose, we double stained sperm suspensions with the Na^+ dye CoroNa Red and propidium iodide to analyze changes in Na^+ in individual live sperm. These experiments show that capacitated sperm are a cell population characterized by lower Na^+ concentrations. This decrease in Na^+ can be blocked by PKA inhibitors and induced by genistein in conditions that do not support sperm capacitation. Moreover, ENaC inhibitors are able to induce a similar Na^+ decrease when added to medium that does not support capacitation. Overall, our observations are consistent with a model in which PKA activation of CFTR inactivates ENaC and consequently induces the capacitation-associated hyperpolarization of the sperm E_m.

Results

Regulation of $[Na^+]_i$ during capacitation

Previously, we presented evidence that Na^+ is involved in determining the sperm plasma membrane resting E_m (Hernandez-Gonzalez et al., 2006). We hypothesized that the contribution of Na^+ to the resting E_m is reduced during capacitation because of downregulation of Na^+ channels such as ENaCs. This possibility was supported by experiments demonstrating that incubation of sperm in non-capacitating medium supplemented with ENaC inhibitors such as amiloride or EIPA was conducive to hyperpolarization. To further investigate this model, $[Na^+]_i$ was measured in individual cells using a flow cytometry approach. Towards this goal, sperm were loaded with the Na^+ probe CoroNa Red, stained with propidium iodide (PI) and analyzed by FACScan, as described in the Materials and Methods section. CoroNa Red was concentrated in the equatorial, postacrosomal compartment (supplementary material Fig. S1A). To discriminate non-sperm particles passing through the flow cytometer detector, two-dimensional sideways (SSC)-forward (FSC) scatter dot plots were used in the absence and in the presence of 0.1% Triton X-100 (Fig. 1A,B). Triton X-100 solubilizes non-sperm particles; therefore, those dot plot events maintained in the presence of detergent were counted as sperm cells. In the following experiments, non-sperm particles presenting scatter properties differing from those of sperm were excluded from the analyses.

Once non-sperm events were excluded, two-dimensional fluorescence dot plots of CoroNa Red (positively correlated with $[Na^+]_i$) versus PI (labeling the DNA of dying cells) were created. These dot blots were used for the analysis of Na^+ concentration in sperm incubated in medium that did not support capacitation (NON, Fig. 1C) or that supported capacitation (CAP, Fig. 1D). A decrease in CoroNa Red fluorescence was observed in capacitated live sperm cells (negative for PI staining) when compared with non-capacitated sperm (Fig. 1E,G). The decrease in CoroNa Red fluorescence was not observed in dead sperm cells (PI positive; Fig. 1E,F). In subsequent experiments, only live sperm population was used for analyses. As a control, to evaluate whether CoroNa Red affected other capacitation-associated parameters, sperm in the same conditions were assayed for the increase in phosphorylation pathways associated with capacitation, as described previously (Krapf et al., 2010). As expected, CoroNa Red did not affect the capacitation-induced increase in phosphorylated PKA substrates (PKAS-*P*) or the increase in phosphorylated tyrosine residues (Y-*P*) as measured with anti-PKAS-*P* or anti-Y-*P* antibodies, respectively (Fig. 1H). Altogether these data are consistent with the hypothesis that capacitation is associated with a blockage in Na^+ transport and the consequent decrease in $[Na^+]_i$. In addition, results using the mitochondria uncoupler CCCP indicate that mitochondria are not involved in the decrease in $[Na^+]_i$ (supplementary material Fig. S1B–E).

During capacitation, a fraction of the sperm population undergoes spontaneous acrosome reaction. To evaluate whether acrosome loss is the cause of reduced $[Na^+]_i$, GFP-Acr transgenic mice were used. Sperm from these mice carry GFP in their acrosomes and this fluorescent protein is lost upon the acrosome reaction (Nakanishi et al., 1999) (Fig. 2A); therefore, the integrity of their acrosome can be easily examined in a non-invasive manner by tracking GFP in individual live sperm by flow cytometry. To analyze $[Na^+]_i$, GFP-Acr sperm were loaded with CoroNa Red as described above, and incubated in medium that supported or did not support capacitation. Similarly to the experiments with sperm from CD1 mice, a decrease in $[Na^+]_i$ upon capacitation was observed only in live GFP-Acr sperm as shown in Fig. 2B (non capacitated) and Fig. 2C (capacitated). To investigate the acrosome status of the sperm population with lower $[Na^+]_i$ in capacitated live sperm, dot plots of GFP versus PI fluorescence were analyzed. Thus, the population of live capacitated sperm could be divided into acrosome-intact (GFP+, in green) and acrosome-reacted (GFP–, in orange) sperm (Fig. 2D). As shown in Fig. 2E, the percentage of sperm with CoroNa Red fluorescence in each of these populations confirmed that the decrease in $[Na^+]_i$ occurred in intact sperm (green histogram) but not in acrosome-reacted, capacitated sperm (orange histogram). These experiments were repeated five times and the results are summarized in Fig. 2F, which shows a

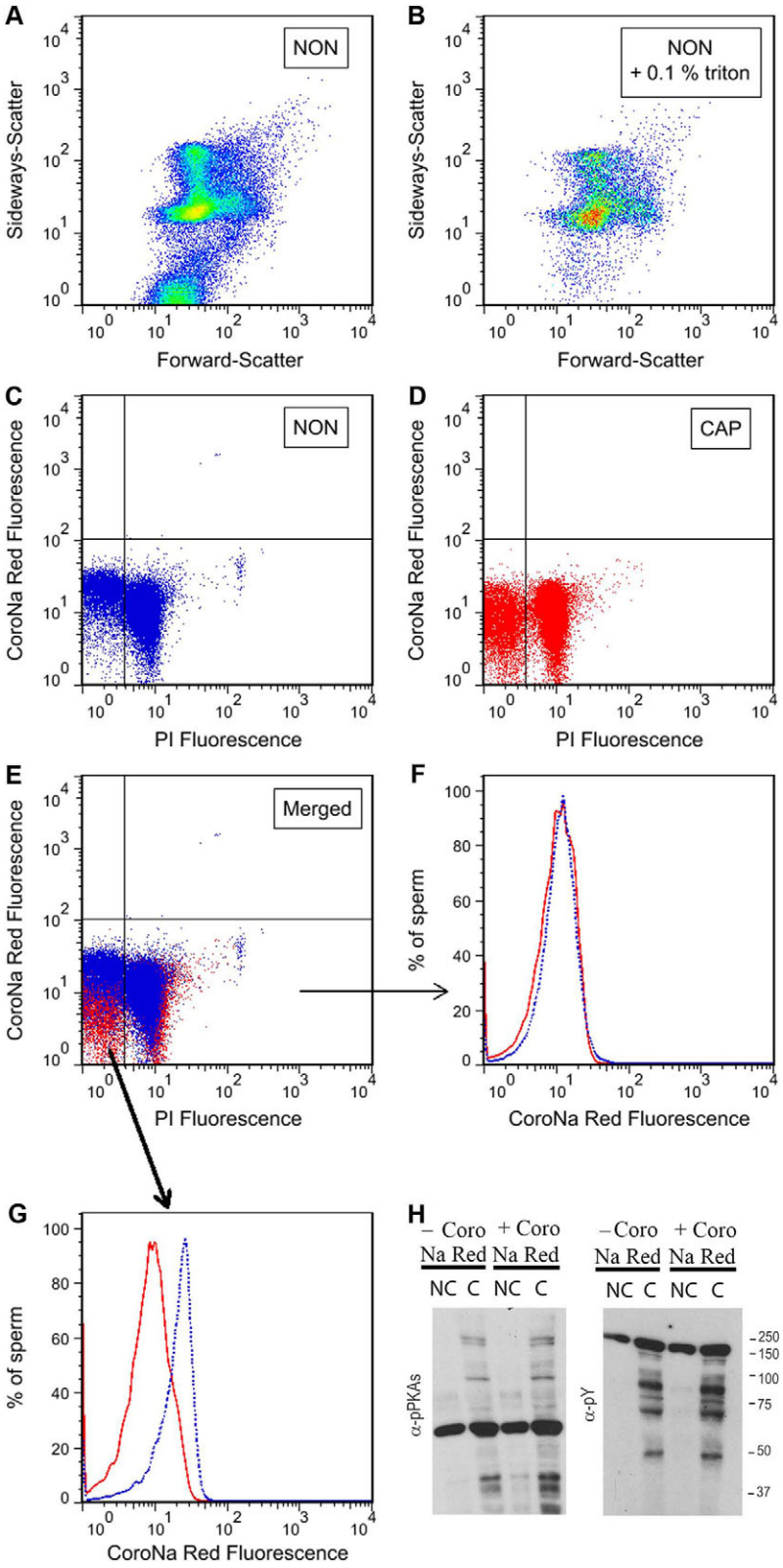

Fig. 1. $[Na^+]_i$ is decreased in live capacitated sperm. Sperm from the cauda epididymus were recovered and loaded with CoroNa Red in medium lacking BSA and HCO_3^-, which does not support capacitation (NON). After 30 minutes incubation, sperm were washed once and resuspended in the same medium or in medium containing BSA and HCO_3^- (CAP). After incubation for 1 hour, PI was added and the sperm population analyzed by flow cytometry. (**A**,**B**) Two-dimensional dot plot sideways-scatter versus forward-scatter analysis of non-capacitated sperm in the absence (A) or in the presence of 0.1% Triton X-100 (B). These analyses made it possible to distinguish between sperm cells and other particles, as explained in the Results. (**C**,**D**) The events involving sperm were then selected for CoroNa Red versus PI two-dimensional fluorescence dot plot analysis of sperm incubated under conditions that did not support (in blue) or supported capacitation (in red). (**E**) Two-dimensional dot plots (as in C and D) were used to distinguish between sperm with low (live) and high (dead) PI staining. Dead (**F**) and live (**G**) sperm populations from the NON (solid red) and CAP (dotted blue) groups were used independently to determine the percentage of sperm showing CoroNa Red fluorescence. (**H**) Sperm incubated in the same media as in A and B were extracted as described and their phosphorylation patterns analyzed with anti-PKAS-*P* and anti-Y-*P* antibodies (α-pPKAs and α-pY).

statistically significant decrease in $[Na^+]_i$ in acrosome-intact, capacitated sperm. As a control, the capacitation-associated increase in phosphorylation was analyzed by western blotting of GFP-Acr sperm extracts (Fig. 2G).

Kinetics and role of a cAMP–PKA pathway in the $[Na^+]_i$ decrease associated with capacitation

To evaluate the kinetics of $[Na^+]_i$ decrease, sperm loaded with CoroNa Red were incubated for different time periods

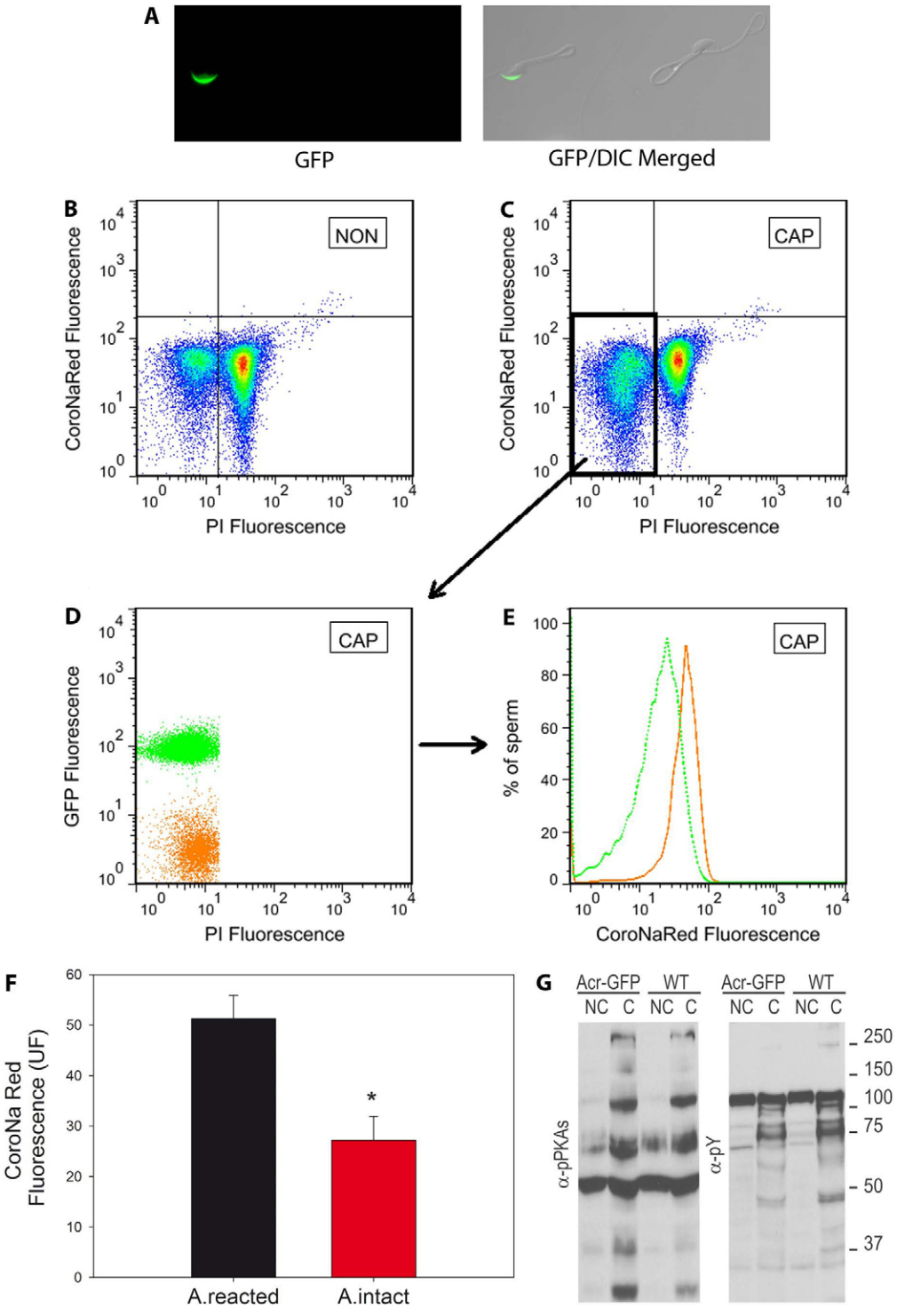

Fig. 2. $[Na^+]_i$ decreases only in acrosomal intact sperm. (**A**) Sperm from the cauda epididymides of Acr-GFP CF1 mice, with GFP in their acrosomes, were incubated in non-capacitating medium. GFP fluorescence (left) and the merged DIC and GFP images (right) of two representative reacted and not-reacted sperm are shown. (**B**,**C**) These sperm were loaded with CoroNa Red for 30 minutes and then incubated in the same medium or in medium that supported capacitation. Before flow cytometry, PI was added to the sperm suspension. Two-dimensional CoroNa Red versus PI fluorescence dot plots of Acr-GFP sperm were used to analyze NON (B) and CAP (C) live and dead sperm as described in Fig. 1. (**D**) The spontaneous acrosome reaction in the capacitated live-sperm population was further analyzed using two-dimensional GFP versus PI dot plots in which two clear populations of cells containing either high GFP (in green), with intact acrosomes, or low GFP (in orange), without acrosomes, can be distinguished. (**E**) These populations were then analyzed and histograms of their individual $[Na^+]_i$ CoroNa Red fluorescence constructed. $[Na^+]_i$ was decreased only in the population with intact acrosomes. (**F**) Average values of CoroNa Red fluorescence in CAP live-sperm populations. Values are means ± s.e.m., $n=5$ (*statistically significant, $P=0.019$, paired t-test). (**G**) Phosphorylation of PKA substrates and tyrosine phosphorylation in wild-type and Acr-GFP sperm was evaluated using western blotting with anti-PKAS-*P* (left panel) and anti-Y-*P* (right panel) antibodies.

(0, 10, 30 and 60 minutes) under conditions that supported capacitation. Analysis of CoroNa Red versus PI dot plots indicates that an increasing number of sperm showed reduced $[Na^+]_i$ over time (Fig. 3A–D). The reduction in CoroNa Red fluorescence over time, averaged from five independent experiments, is shown in Fig. 3E. This decrease was compared with the kinetics of phosphorylation of PKA substrates as well as phosphorylation in tyrosine residues (Fig. 3F). It is noteworthy that a maximum decrease in $[Na^+]_i$ occurred at 30 minutes, whereas maximum PKA activation occurred much earlier (Fig. 3) (Morgan et al., 2008). This observation is consistent with the idea that a cAMP–PKA pathway is upstream of Na^+ transport regulation.

To investigate the role of this pathway in the regulation of $[Na^+]_i$, sperm loaded with CoroNa Red were incubated in media that supported or did not support capacitation (Fig. 4A,B). Moreover, in order to directly stimulate PKA, sperm were also incubated in medium that did not support capacitation that

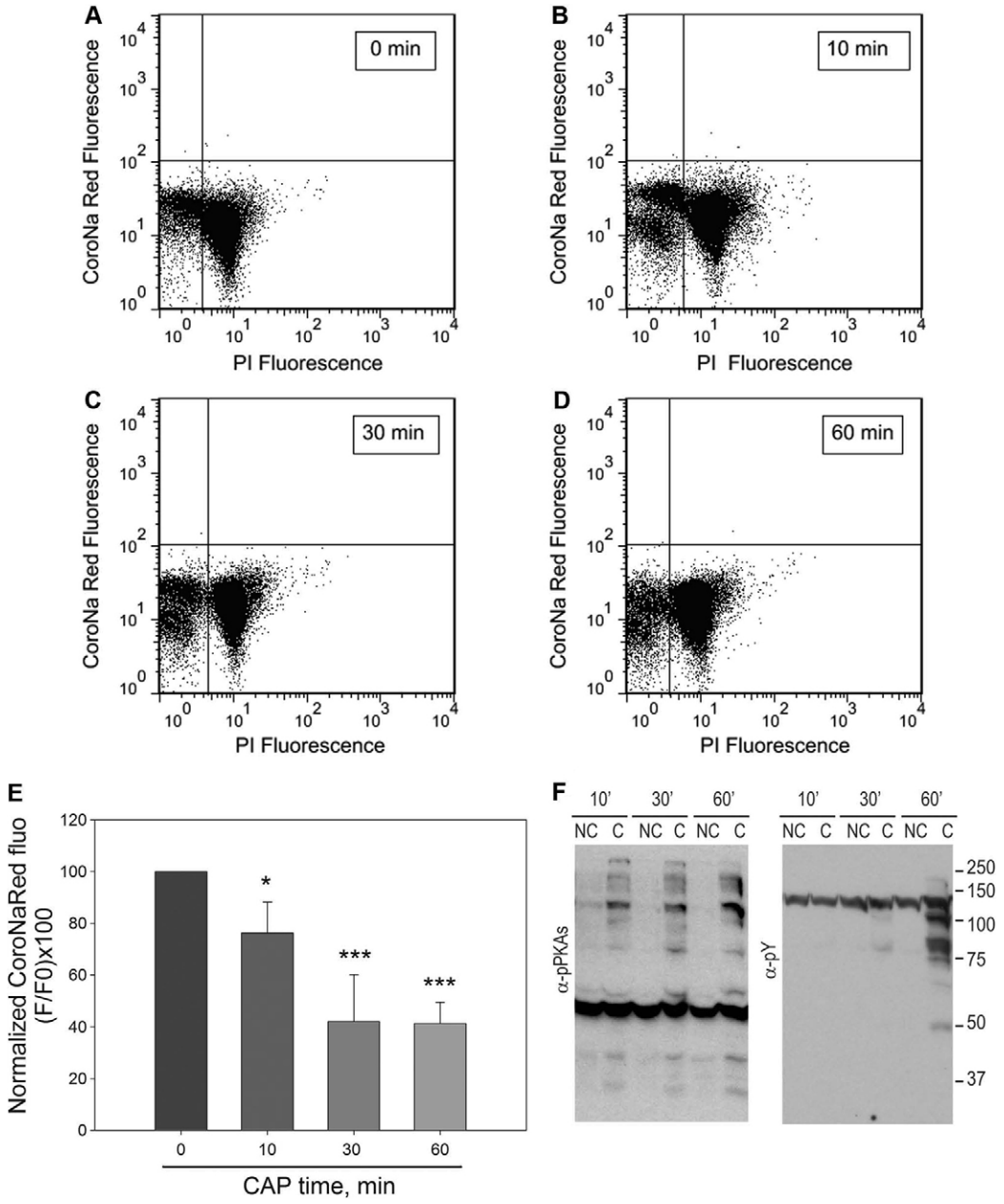

Fig. 3. Decrease in $[Na^+]_i$ occurs after activation of PKA and before the increase in tyrosine phosphorylation. Sperm from the cauda epididymus were loaded with CoroNa Red, as described, for 30 minutes, then washed and incubated for different time periods in medium that supported capacitation. (**A–D**) Two-dimensional fluorescence dots plots of CoroNaRed versus PI of sperm incubated for 0 (A), 10 (B), 30 (C) and 60 (D) minutes. (**E**) CoroNa Red fluorescence in the live sperm population at each time point. Values are means ± s.e.m. (n=5, *P≤0.05 and **P≤0.01). (**F**) Western blots, using anti-PKAS-*P* (left panel) and anti-Y-*P* (right panel), of sperm extracts incubated for different time periods in the same media that were used for flow cytometry experiments.

included cAMP agonists (1 mM db-cAMP in combination with the broad-spectrum phosphodiesterase inhibitor IBMX at 100 μM; Fig. 4C). In these conditions, cAMP agonists decrease $[Na^+]_i$ suggesting that activation of a cAMP–PKA pathway is sufficient to induce $[Na^+]_i$ decrease. The normalized mean fluorescence from four independent experiments is summarized in Fig. 4D. In each condition, the phosphorylation status of PKA substrates and tyrosine-phosphorylated proteins were analyzed by western blotting (Fig. 4E).

To further investigate the role of the cAMP pathway, sperm were loaded with CoroNa Red as described above and incubated in medium that did not support (Fig. 5A,D, NON) or supported capacitation, either in the absence (Fig. 5B,D, CAP) or in the presence of increasing concentrations of the PKA inhibitor H-89 (Fig. 5C,D, H-89). The effect of increasing concentrations of H-89 on $[Na^+]_i$ was evaluated using the mean fluorescence obtained from five independent experiments (Fig. 5D). The effect of this PKA inhibitor was also evaluated by detecting phosphorylated PKA

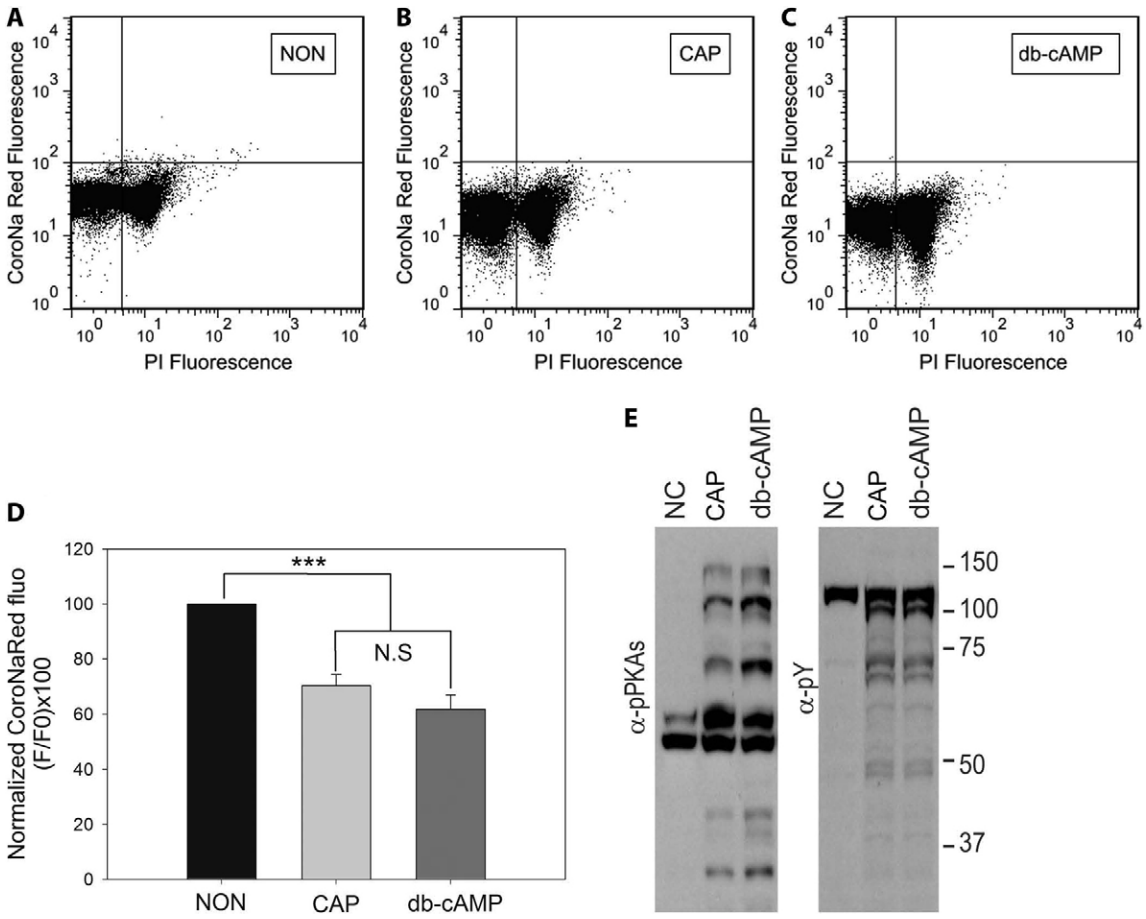

Fig. 4. Decrease in $[Na^+]_i$ is regulated by a cAMP-PKA-dependent pathway. Sperm from the cauda epididymus were placed in medium without HCO_3^-, which does not support capacitation, loaded for 30 minutes with CoroNa Red and washed as described. Aliquots of sperm suspension were incubated in the media described below for an additional hour. (**A–C**) Two-dimensional dot plots of PI versus CoroNa Red fluorescence of sperm incubated in non-capacitating medium (A, NON), in medium that supported capacitation (B, CAP) and, in order to directly stimulate PKA, sperm were also incubated in medium that did not support capacitation, i.e. with cAMP agonists (1 mM db-cAMP in combination with 100 μM IBMX; C, cAMP). (**D**) Quantification of CoroNa Red fluorescence of cells in A–C. Values are means ± s.e.m., $n=4$ (***$P\leq0.001$). (**E**) Western blots, using anti-PKAS-*P* (left panel) and anti-Y-*P* (right panel) antibodies, of sperm extracts incubated as in A–C.

substrates and tyrosine-phosphorylated proteins in western blots (Fig. 5E). Altogether, results shown in Figs 3, 4 and 5 indicate that the decrease in $[Na^+]_i$ is downstream a cAMP–PKA pathway.

Amiloride, EIPA and genistein decrease $[Na^+]_i$

Previously, we have shown that amiloride and EIPA are capable of hyperpolarizing sperm E_m in conditions that do not support capacitation (Hernandez-Gonzalez et al., 2006), suggesting that ENaCs are involved in the regulation of capacitation-associated hyperpolarization of the sperm plasma membrane. To investigate whether the overall decrease in Na^+ observed using flow cytometry analysis was mediated by amiloride-sensitive Na^+ channels, sperm were loaded with CoroNa Red and then incubated in conditions that did not support capacitation in the absence (Fig. 6A) or in the presence of increasing concentrations of amiloride (Fig. 6B,E) or EIPA (Fig. 6C,F). Four independent experiments were performed, and $[Na^+]_i$ was analyzed as shown in Fig. 6E,F. Our findings indicate that the amiloride- or EIPA-induced decrease in $[Na^+]_i$ is consistent with the effect of these compounds on the resting sperm plasma E_m (Hernandez-Gonzalez et al., 2006).

CFTR is a Cl^- channel modulated by a cAMP–PKA pathway (Chang et al., 2002; Lu et al., 2010). We have previously shown that CFTR inhibitors block the capacitation-associated E_m hyperpolarization in sperm. Moreover, activation of CFTR by genistein is able to induce hyperpolarization in sperm incubated under non-capacitating conditions. To evaluate whether $[Na^+]_i$ is affected by CFTR activation, sperm loaded with CoroNa Red were incubated in non-capacitating medium in the absence (Fig. 7A,D) or in the presence of genistein (Fig. 7B,D). Consistent with a role of CFTR upstream of Na^+ transport, genistein decreased the mean fluorescence of the sperm population to levels similar to those obtained in capacitated sperm populations (Fig. 7C,D). The highest genistein concentration used for these experiments did not affect the increase in phosphorylation of either PKA substrates or of tyrosine residues (Fig. 7E). To further explore the role of Cl^- transport in the regulation of $[Na^+]_i$, sperm were incubated with all the compounds needed for capacitation in the presence (Fig. 7F,H) or in the absence of Cl^- (Fig. 7G,H). In these conditions, the decrease in $[Na^+]_i$ was significantly ($P<0.0005$) decreased (Fig. 7I). The role of CFTR in the regulation of $[Na^+]_i$

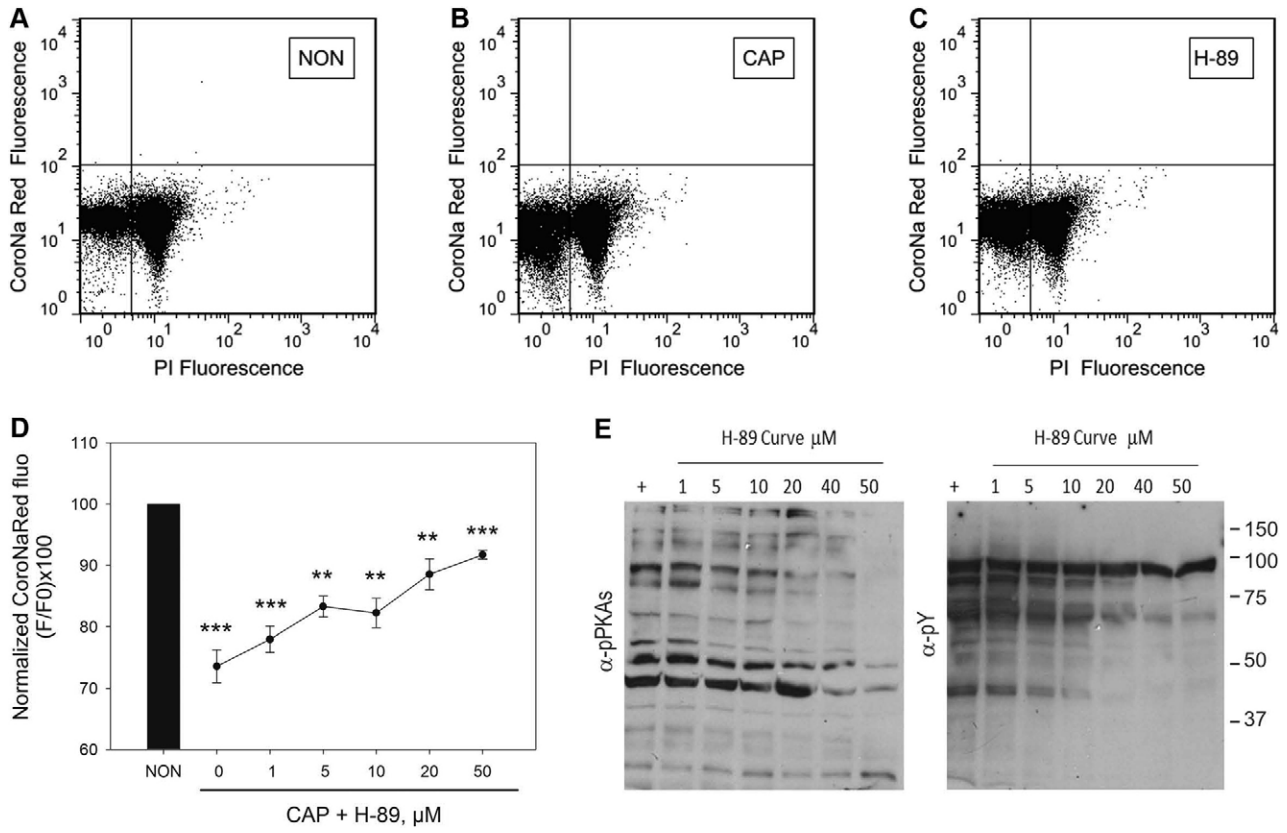

Fig. 5. PKA inhibition by H-89 blocks the capacitation-associated decrease in $[Na^+]_i$. (**A–D**) Sperm from the cauda epididymus were placed in medium that did not support capacitation, which was loaded with CoroNa Red for 30 minutes, washed and incubated in the same medium (NON; A) or in medium that supported capacitation (CAP; B) in the absence or in the presence of increasing concentrations of H-89 (0, 1, 5, 10, 20 and 50 µM; C and D). (A–C) Two-dimensional dot plots of PI versus CoroNa Red fluorescence of sperm incubated under non-capacitating (NON) or under capacitating (CAP) conditions in the absence or in the presence of 50 µM H-89. (D) CoroNa Red fluorescence. Values are means ± s.e.m. from four independent experiments (**$P \leq 0.01$; ***$P \leq 0.001$). (**E**) Western blots, using anti-PKAS-*P* (left panel) and anti-Y-*P* (right panel) of sperm extracts incubated in the same media as the ones used for the flow cytometry.

was also investigated by testing the CFTR inhibitor CFTR(inh)-172. We noted that this compound affected the forward-scatter vs sideways-scatter two-dimensional dot plots suggesting that CFTR inhibitors have an effect on sperm morphology (data not shown). Therefore, it was not possible to evaluate changes in $[Na^+]_i$ concentration when CFTR(inh)-172 was present under the conditions used in our flow cytometry analyses.

Discussion

In mammalian sperm, the ability to fertilize is achieved in the female tract in a process known as capacitation. Capacitation is associated with the activation of a PKA-dependent pathway and with a downstream increase in protein tyrosine phosphorylation. In addition, capacitation is also associated with hyperpolarization of the sperm plasma E_m in some mammalian species such as mouse and horse (Arnoult et al., 1999; Hernandez-Gonzalez et al., 2006; McPartlin et al., 2011). Differences in the concentration of ions between the intracellular and extracellular milieu determine the cell resting E_m. Before capacitation, mouse sperm have an E_m of approximately –35 mV; this relatively depolarized E_m suggests that Na^+ ions contribute to the setting of the sperm E_m. We have shown that replacing Na^+ by non-permeable cations hyperpolarizes sperm E_m. Moreover, addition of Na^+ to sperm incubated in Na^+-free medium resulted in depolarization of their plasma E_m (Hernandez-Gonzalez et al., 2006) suggesting that an electrogenic Na^+ uptake system is present and active in mouse sperm. Moreover, we have previously shown that: (1) this electrogenic Na^+ permeability is blocked by amiloride and its analogue EIPA; (2) it is activated by external acidification ($pH_e < 7.4$); (3) it has an ion selectivity of $Li^+ > Na^+ > Cs^+$ or K^+; and (4) ENaC subunits α and δ are present in mature mouse sperm. Altogether, this evidence suggested that before capacitation, ENaC channels are involved in the regulation of the sperm resting E_m. In addition, the observation that the amiloride-sensitive Na^+-induced depolarization is substantially reduced in a capacitated sperm population is consistent with the hypothesis that the capacitation-associated hyperpolarization is due, at least in part, to ENaC closing (Hernandez-Gonzalez et al., 2006).

More recently, our group, as well as others has demonstrated that Cl^- ions are also essential for capacitation. Replacement of Cl^- with non-permeable anions results in the inhibition of the capacitation-associated increase in tyrosine phosphorylation and hyperpolarization of the sperm plasma E_m (Hernandez-Gonzalez et al., 2007; Wertheimer et al., 2008). As mentioned in the introduction, work by our group as well as others demonstrated

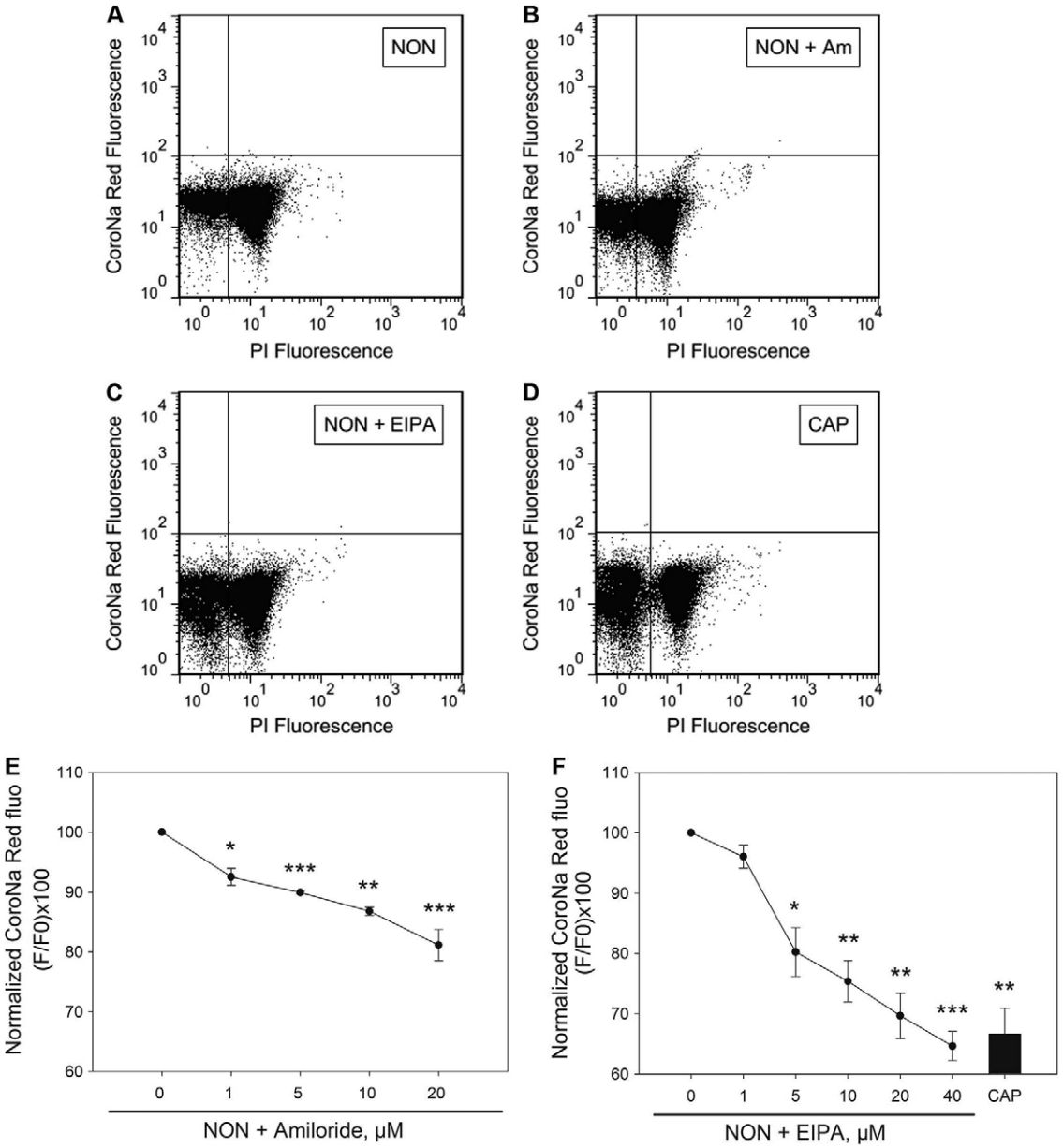

Fig. 6. Amiloride and EIPA induced a decrease in $[Na^+]_i$ in non-capacitated sperm. Sperm from the cauda epididymus were placed in medium that did not support capacitation, loaded with CoroNa Red, washed and incubated for an additional 60 minutes in the absence or in the presence of increasing concentrations of amiloride and EIPA. (**A–C**) Representative two-dimensional dot plots of PI versus CoroNa Red fluorescence of sperm incubated in the absence (NON) or in the presence of amiloride (Am) and EIPA (20 and 40 μM, respectively). (**E**,**F**) CoroNa Red fluorescence of live sperm that were incubated with increasing concentrations of amiloride (E) or EIPA (F) in non-capacitating conditions. Values are means ± s.e.m. of four independent experiments (**$P \leq 0.01$; ***$P \leq 0.001$). A bar represents the value for the capacitated live sperm population.

the presence of CFTR in mammalian sperm (Hernandez-Gonzalez et al., 2007; Xu et al., 2007). Our results indicate that: (1) CFTR inhibitors such as DPC (diphenylamine-2-carboxylic acid) block the capacitation-associated hyperpolarization in mouse sperm; (2) activation of this channel with genistein in medium that did not support capacitation induced hyperpolarization; and (3) CFTR protein is present in the sperm. Our working hypothesis is that activation of a cAMP–PKA pathway during capacitation stimulates CFTR and that this stimulation is coupled to the inhibition of Na^+ transport by ENaC. Interestingly, both ENaC α and CFTR were shown to localize to the sperm mid-piece (Hernandez-Gonzalez et al., 2006; Hernandez-Gonzalez et al., 2007).

What is the function of the capacitation-associated hyperpolarization? It has been proposed that because capacitation prepares sperm for the acrosome reaction, capacitation-associated membrane hyperpolarization might regulate the ability of sperm to generate transient Ca^{2+} elevations during acrosome reaction by physiological agonists (e.g. egg zona pellucida or progesterone) (Florman et al., 1998). Which is the Ca^{2+} channel responsible for the agonist-induced acrosome reaction is controversial at present. Although the low

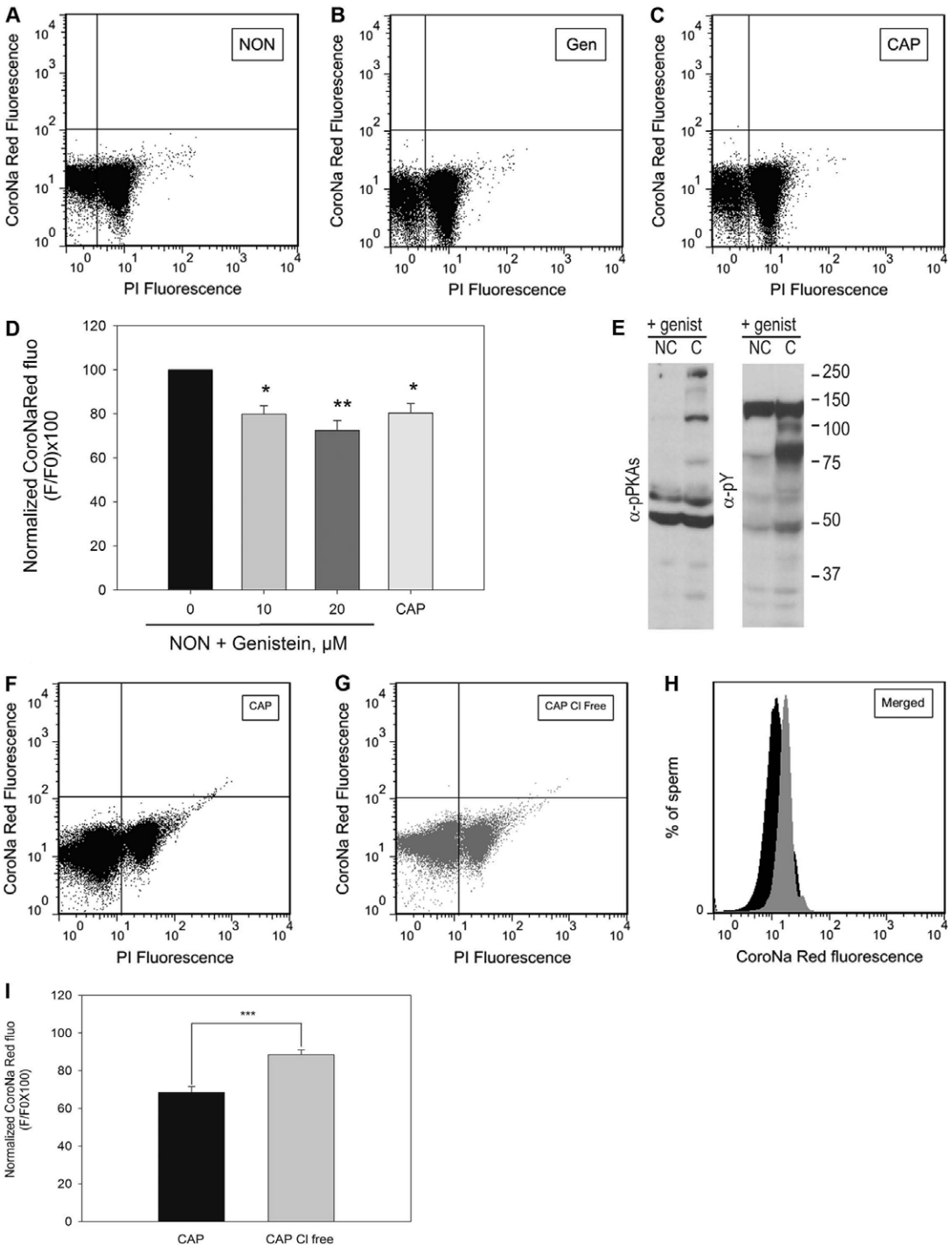

Fig. 7. Decrease in $[Na^+]_i$ is induced by genistein in non-capacitated sperm and blocked in the absence of Cl^- in capacitated sperm. Sperm from the cauda epididymus placed in non-capacitating medium were loaded with CoroNa Red for 30 minutes, washed and then incubated for an additional hour in the same medium in the absence or presence of increasing concentrations of genistein. Another aliquot was incubated for 60 minutes in complete medium. (**A–C**) Two-dimensional dot plots of PI versus CoroNa Red fluorescence of sperm incubated in non-capacitating (NON; A), non-capacitating and 20 µM genistein (Gen; B) or in capacitating (CAP; C) media. (**D**) Normalized CoroNa Red fluorescence of live sperm that were incubated with increasing concentrations of genistein. Values are means ± s.e.m. of four independent experiments. (**E**) Western blots, using anti-PKAS-*P* and anti-Y-*P*, of sperm extracts incubated in medium that supported (CAP) or did not support (NC) capacitation, in the presence of 20 µM genistein. (**F**,**G**) Two-dimensional dot plots of PI versus CoroNa Red fluorescence of sperm in medium that supported capacitation, in the presence (CAP; F) or in the absence of Cl^- (CAP, Cl^- free; G). (**H**) The percentage of live sperm showing CoroNa Red fluorescence in CAP and CAP Cl^--free media. (**I**) Normalized CoroNa Red fluorescence of live sperm that were incubated in medium that supported capacitation, in the presence (CAP) or in the absence of Cl^- (Cap Cl^- free). Values are means ± s.e.m. of eight independent experiments (**P*≤0.05; ***P*≤0.01; ****P*≤0.001).

voltage-activated Ca_v3 Ca^{2+} T-channels has been measured in spermatogenic cells (Arnoult et al., 1996; Escoffier et al., 2007; Lievano et al., 1996) and in mouse testicular sperm (Martinez-Lopez et al., 2009), no Ca_v currents have been detected in epididymal sperm (Ren and Xia, 2010). Also, it should be considered that $Ca_v3.1$ and $Ca_v3.2$ null mice are fertile, suggesting that neither of these channels alone is essential for sperm function (Escoffier et al., 2007). Although the role of Ca_v channels has not been established, it has been shown that sperm incubated under conditions that blocked hyperpolarization failed to undergo the ZP-induced acrosome reaction (Acevedo et al., 2006; Munoz-Garay et al., 2001; Zeng et al., 1995). As an alternative possibility, hyperpolarization could be needed to remove inactivation of another type of calcium channel, to increase the driving force for Ca^{2+} uptake or for other aspects of capacitation. More experiments are needed to elucidate this pathway.

Reduction of $[Na^+]_i$ during capacitation correlates with the observed hyperpolarization. However, the sperm plasma E_m also depends on the equilibrium state of other ions in the capacitation medium. In particular, it has been shown that opening of a K^+ channel contributes to sperm plasma E_m hyperpolarization during capacitation. In particular, an inward rectifying K^+ current is present in spermatogenic cells. This inward rectifying K^+ current is sensitive to Ba^{2+}, tolbutamide and glibenclamide (Acevedo et al., 2006; Munoz-Garay et al., 2001); these compounds are also able to block the capacitation-associated hyperpolarization, suggesting the participation of this type of K^+ channels in this process. Recently, SLO3, a sperm-specific K^+ channel (Schreiber et al., 1998) was knocked out in mice. These mice are sterile and their sperm do not undergo hyperpolarization during capacitation (Santi et al., 2010). In addition, sperm from the SLO3 knock-out mice are not able to undergo the ZP-induced acrosome reaction. More interestingly, if hyperpolarization is induced pharmacologically by adding valinomycin, the SLO3 knock-out sperm recover their acrosome reaction in the presence of ZP. This result suggests that hyperpolarization is necessary for the acrosome reaction (Santi et al., 2010). It is yet not known how SLO3, either directly or indirectly, participates in the physiological regulation of the sperm plasma E_m. However, sperm from *Slo3* null mice do not undergo alkalinization-stimulated hyperpolarization (Zeng et al., 2011).

When considering the ZP-induced acrosome reaction as an endpoint of capacitation, it has been observed that in most species, not every sperm within a population capacitates in vitro. In the mouse, this was determined by evaluating the percentage of the ZP-induced acrosome reaction (Arnoult et al., 1999; Visconti et al., 1995a). Following these criteria, fewer than 50% of sperm are capacitated after 1.5 hours incubation in a complete medium. Because capacitation is associated with the sperm E_m hyperpolarization, it has been hypothesized that only the capacitated population shows these changes (Arnoult et al., 1999). This possibility could be evaluated using a cell sorting approach. Flow cytometry has become widely used for sperm analysis, replacing, in many cases, time-consuming and more error-prone methods. Flow cytometry allows the analysis of thousands of cells within seconds, capturing many of their individual features with a reproducibility not possible by other methods. Initially, flow cytometry of sperm was used in conjunction with DNA staining dyes; these experiments were designed to explore chromosomal content of a normal sperm population of cell bearing both X and Y chromosomes (Van Dilla et al., 1977). These initial experiments formed the basis for sexing mammalian sperm and the strategy was applied later to predetermine sex in livestock offspring (Johnson, 2000). In addition, several fluorescent probes have been used for the analysis of viability, mitochondrial E_m, apoptotic markers and sperm size (reviewed by Martinez-Pastor et al., 2010).

In the present work, we used the Na^+ dye CoroNa Red to analyze the extent of $[Na^+]_i$ changes within a mouse sperm population undergoing capacitation by flow cytometry. The central observations of this study are that: (1) as part of capacitation, a significant portion of the live sperm population decreased their $[Na^+]_i$, resulting in a significant reduction of the mean fluorescence of CoroNa Red; (2) neither capacitating conditions nor any of the inhibitors assessed affected $[Na^+]_i$ in PI-positive cells (i.e. dead sperm); (3) a decrease in $[Na^+]_i$ was observed only in sperm with intact acrosomes; (4) the decrease in $[Na^+]_i$ is downstream of PKA activation as determined using cAMP agonists and H-89; (5) amiloride, EIPA and genistein decreased $[Na^+]_i$ in sperm incubated in medium that did not support capacitation. Altogether these results are consistent with a model in which activation of CFTR by a cAMP–PKA pathway blocks ENaC with the consequent decrease in $[Na^+]_i$ and hyperpolarization of the sperm E_m (Fig. 8). In this model, bicarbonate transport activates the atypical sperm adenylyl cyclase with the subsequent increase in cAMP levels and PKA activity. PKA activation upregulates Cl^- transport through CFTR; either Cl^- transport or conformational changes in CFTR are then coupled to inactivation of ENaC. This inactivation results in decreased electrogenic Na^+ transport with the consequent E_m hyperpolarization. This part of the model in Fig. 8 is consistent with a role of Na^+ in the regulation of the sperm E_m. As mentioned above, sperm from *Slo3* null mice are not hyperpolarized during capacitation; therefore, it appears that these channels are involved in the regulation of the sperm E_m. Whether the role of these channels is direct, through outward K^+ influx, or indirect, through an unknown regulatory mechanism, has not been established yet.

The conclusion that $[Na^+]_i$ is decreased during capacitation was derived from the analysis of the mean CoroNa Red fluorescence in the sperm population. Alternatively, our results could indicate that different fractions of the sperm population behave differently in terms of their $[Na^+]_i$. Although a significant percentage of sperm show a decrease in $[Na^+]_i$, another fraction maintains it at high levels. These observations warrant future investigations on whether different capacitation-associated changes could occur in the same sperm population. For this purpose, the fluorescent dyes should comply with the following criteria: (1) the loading procedure should be compatible with live sperm; (2) fluorescence levels should be sensitive enough to allow a clear separation of at least two sperm populations; and (3) the parameter under study should be correlated with capacitation. In addition, the use of different fluorescent probes can be combined to evaluate more than one capacitation-related parameter simultaneously. For example in this work, using sperm from GFP-Acr mice, the sperm acrosome status was correlated with CoroNa Red fluorescence. These experiments indicated that only the acrosome-intact sperm had lower $[Na^+]_i$. Correlation of $[Na^+]_i$ with other capacitation-associated parameters will allow further investigation on the molecular mechanisms involved in the regulation of sperm capacitation.

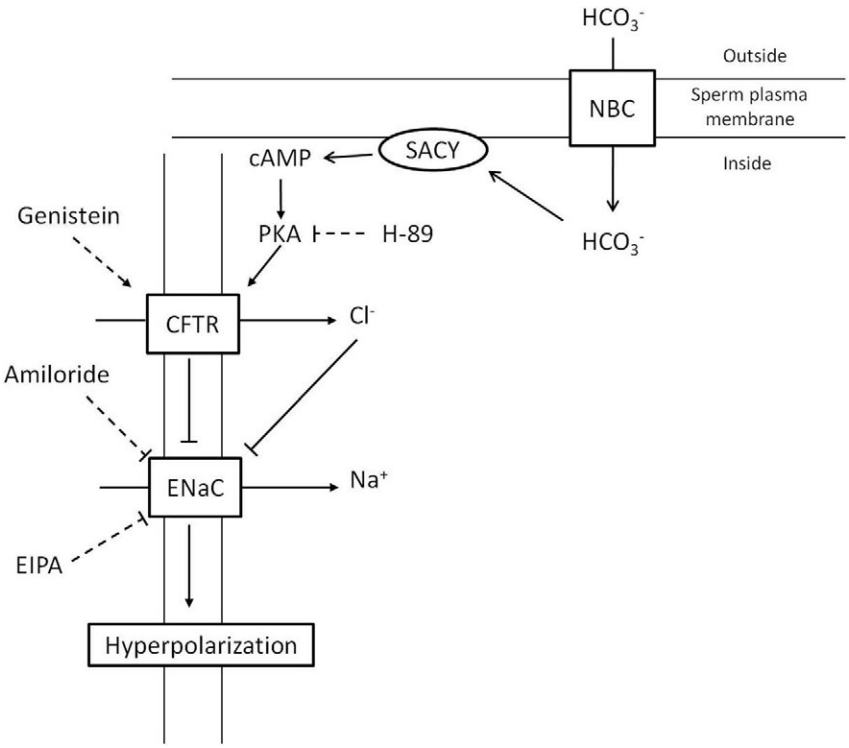

Fig. 8. Capacitation-associated hyperpolarization model. We propose that $[Na^+]_i$ is decreased when sperm are incubated under conditions that support capacitation. This decrease is blocked by amiloride and stimulated by genistein, a CFTR activator, and also by cAMP agonists. Taking this information into consideration, our working hypothesis postulates that the increase in cAMP levels that accompany capacitation is responsible for CFTR activation with the consequent inhibition of ENaC and the hyperpolarization of the sperm E_m. SACY, soluble adenylyl cyclase.

Materials and Methods

Materials

Chemicals were obtained from the following sources: bovine serum albumin (BSA; fatty acid-free), dibutyryl-cAMP (Bt2cAMP), 3-isobutyl-1-methylxanthine (IBMX), 4-bromo-calcium ionophore A23187, amiloride hydrochloride hydrate, 5-(*N*-ethyl-*N*-isopropyl) amiloride (EIPA), sodium gluconate and carbonyl cyanide *m*-chlorophenylhydrazone (CCCP) were from Sigma (St Louis, MO); H-89 was from Cayman Chemical Company (Ann Arbor, MI); rabbit monoclonal anti-phosphorylated PKA substrate (clone 100G7E) was purchased from Cell Signaling (Danvers, MA); anti-phosphorylated tyrosine (Y-*P*) monoclonal antibody (clone 4G10) was from Upstate Biotechnology (Lake Placid, NY); horseradish peroxidase-conjugated anti-mouse and anti-rabbit IgG were purchased from Jackson ImmunoResearch Laboratories (West Grove, PA) and GE Life Sciences, respectively; propidium iodide and CoroNaRed sodium fluorescent probes were from Invitrogen.

Mouse sperm preparation

CD1 retired male breeders (Charles River Laboratories, Wilmington, MA), and Acr-GFP transgenic male mice (7- to 8-weeks old) were used, in accordance with IACUC of the University of Massachusetts-Amherst guidelines. The Acr-GFP CF1 is a transgenic mouse line that accumulates mutated green fluorescent protein (EGFP) in the sperm acrosome (Nakanishi et al., 1999). Sperm were obtained by manually triturating cauda epididymides in 1 ml of Whitten's HEPES-buffered medium. This medium does not support capacitation unless supplemented with 5 mg/ml bovine serum albumin (BSA; fatty acid-free) and 15 mM $NaHCO_3$. After 10 minutes, the fraction of motile sperm was diluted four times in the appropriate medium depending on the experiment performed. For capacitation, $NaHCO_3$ and BSA were added to final concentrations of 15 mM and 5 mg/ml, respectively. Sperm were incubated in capacitation medium at 37℃ for different time periods depending on the experimental design. To test the effect of different compounds (e.g. genistein and H-89), sperm were preincubated with inhibitors in non-capacitating medium for 15 minutes before the beginning of the capacitating period. To investigate the role of Cl^- in the capacitation medium, sperm were incubated in capacitation medium without or with Cl^- ions. Cl^- was replaced by the non-permeant anion gluconate as previously described (Wertheimer et al., 2008). The contribution of mitochondrial membrane potential was evaluated using the mitochondrial uncoupler CCCP as described previously (Demarco et al., 2003).

SDS-PAGE and immunoblotting

Western blots were conducted as previously described (Krapf et al., 2010). Briefly, after treatment, sperm were collected by centrifugation, washed in 1 ml phosphate-buffered saline, resuspended in Laemmli sample buffer without β-mercaptoethanol, and boiled for 5 minutes. After centrifugation, 5% β-mercaptoethanol was added to the supernatants, and the mixture was boiled again for 5 minutes. Protein extracts equivalent to $1–2x \times 10^6$ sperm were loaded per lane and subjected to SDS-PAGE and electro-transfer to PVDF membranes (Bio-Rad) at 250 mA for 60 minutes on ice. Membranes were treated with 5% fat-free milk in Tris-buffered saline (TBS) containing 0.1% Tween 20 (T-TBS) for anti-PKA-*P* immunodetections and with 20% fish skin gelatin (Sigma) in T-TBS for anti-Y-*P* immunodetections. Antibodies were diluted in T-TBS as follows: 1/10,000 for anti-Y-*P* (clone 4G10), 1/5000 for anti-PKA-*P* (clone 100G7E). After incubation with secondary antibodies (1/10,000 in T-TBS), enhanced chemiluminescence detection kit (ECL plus, Amersham Biosciences) was used according to the manufacturer's instructions. Hexokinase, a protein known to be constitutively phosphorylated on tyrosine residues, served as a loading control. When necessary, PVDF membranes were stripped at 65℃ for 15 minutes in 2% SDS, 0.74% β-mercaptoethanol, 62.5 mM Tris, pH 6.5, and washed six times for 5 minutes each in T-TBS. For all experiments, molecular masses are expressed in kDa.

Sperm analysis by flow cytometry

Sperm from cauda epididymides were allowed to swim in Whitten's HEPES-buffered medium for 10 minutes. These sperm were loaded with 1 μM CoroNa Red sodium indicator by incubation for 30 minutes at 37℃ in Whitten's HEPES-buffered medium. To eliminate any unincorporated dye, sperm suspensions were then centrifuged (5 minutes, 70 ***g***). Pellets were then resuspended in Whitten's HEPES-buffered medium with or without 15 mM $NaHCO_3$ and 5 mg/ml BSA and incubated for 60 minutes at 37℃. To test the effect of different compounds (e.g. genistein and H-89), sperm were incubated with the respective compound for 15 minutes before incubation in capacitating medium. Before assaying the sperm by flow cytometry, sperm suspensions were filtered through a 100-μm nylon mesh (Small Parts, Inc., Seattle, WA), and 2.1 μM of propidium iodide (PI) was added. Analyses were conducted using a LSR II flow cytometer (Becton Dickinson, San Jose, CA). CoroNa Red, PI and GFP were excited using a 488-nm argon excitation laser. Nonviable cells became PI positive, and their red fluorescent signal detected as fluorescence of wavelength >670 nm. Orange fluorescence from CoroNa-Red-positive cells was detected at 561–606 nm. Finally, sperm cells with intact acrosomes remained GFP positive, and their green fluorescence was detected at 515–545 nm. The three dyes had minimal emission overlap. Roederer guidelines (available at http://www.drmr.com/compensation) were used for compensations. Non-sperm events were gated out from analyses by judging the scatter properties of the events as detected in the forward-scatter and sideways-scatter detector respectively (scatter-gated sperm analysis). Recording of scatter and fluorescent properties of all events stopped when 50,000 events were reached. Two-dimensional plots of sideways- and forward-scatter properties as well as of PI

fluorescence or GFP versus CoroNa Red fluorescence were obtained using FlowJo v7.6 software. Average values of CoroNa Red fluorescence were calculated using the equation $(F/F_0) \times 100$, where F_0 is the CoroNa Red fluorescence from live sperm incubated for 1 hour in non-capacitating medium that does (NON) and F is the fluorescence from sperm in the respective experimental condition (e.g. genistein, amiloride, capacitating conditions, etc).

Fluorescence microscopy analysis

To verify staining patterns of GFP-positive acrosomes and CoroNa Red, sperm suspensions were fixed with 4% of PFA and then mounted on a slide, as previously described (Escoffier et al., 2010a). Fluorescence images of sperm were captured with a Zeiss Axiovert 200M microscope fitted with a ×60 oil immersion objective and a Hamamatsu Orca-AG cooled CCD camera controlled by AxioVision software 4.6 (Zeiss).

Statistics

Statistical analyses were performed using SigmaPlot (version 10). In order to account for variability in sperm samples between males, we used a paired *t*-test. Values are means ± s.e.m. *P*-values of ≤0.05, ≤0.01 or ≤0.001 were considered statistically significant.

Acknowledgements

We thank Eva Wertheimer for helpful advice and Ana Maria Salicioni for critical reading of this manuscript.

Funding

This work was supported by Dirección General Asuntos del Personal Académico, Universidad Nacional Autónoma de México (UNAM) [grant number IN225406 to A.D.]; Consejo Nacional de Ciencia y Tecnología, México (CONACyT) [grant number 128566 to A.D.]; and National Institutes of Health [grant numbers R01 HD44044 to P.E.V., and HD038082 to P.EV. and A.D.]. Deposited in PMC for release after 12 months.

Supplementary material available online at
http://jcs.biologists.org/lookup/suppl/doi:10.1242/jcs.093344/-/DC1

References

Acevedo, J. J., Mendoza-Lujambio, I., de la Vega-Beltran, J. L., Trevino, C. L., Felix, R. and Darszon, A. (2006). KATP channels in mouse spermatogenic cells and sperm, and their role in capacitation. *Dev. Biol.* **289**, 395-405.

Arcelay, E., Salicioni, A. M., Wertheimer, E. and Visconti, P. E. (2008). Identification of proteins undergoing tyrosine phosphorylation during mouse sperm capacitation. *Int. J. Dev. Biol.* **52**, 463-472.

Arnoult, C., Cardullo, R. A., Lemos, J. R. and Florman, H. M. (1996). Activation of mouse sperm T-type Ca^{2+} channels by adhesion to the egg zona pellucida. *Proc. Natl. Acad. Sci. USA* **93**, 13004-13009.

Arnoult, C., Lemos, J. R. and Florman, H. M. (1997). Voltage-dependent modulation of T-type calcium channels by protein tyrosine phosphorylation. *EMBO J.* **16**, 1593-1599.

Arnoult, C., Kazam, I. G., Visconti, P. E., Kopf, G. S., Villaz, M. and Florman, H. M. (1999). Control of the low voltage-activated calcium channel of mouse sperm by egg ZP3 and by membrane hyperpolarization during capacitation. *Proc. Natl. Acad. Sci. USA* **96**, 6757-6762.

Austin, C. R. (1952). The capacitation of the mammalian sperm. *Nature* **170**, 326.

Buffone, M. G., Foster, J. A. and Gerton, G. L. (2008). The role of the acrosomal matrix in fertilization. *Int. J. Dev. Biol.* **52**, 511-522.

Canessa, C. M., Schild, L., Buell, G., Thorens, B., Gautschi, I., Horisberger, J. D. and Rossier, B. C. (1994). Amiloride-sensitive epithelial Na^+ channel is made of three homologous subunits. *Nature* **367**, 463-467.

Chang, M. C. (1951). Fertilizing capacity of spermatozoa deposited into the fallopian tubes. *Nature* **168**, 697-698.

Chang, S. Y., Di, A., Naren, A. P., Palfrey, H. C., Kirk, K. L. and Nelson, D. J. (2002). Mechanisms of CFTR regulation by syntaxin 1A and PKA. *J. Cell Sci.* **115**, 783-791.

de Vries, K. J., Wiedmer, T., Sims, P. J. and Gadella, B. M. (2003). Caspase-independent exposure of aminophospholipids and tyrosine phosphorylation in bicarbonate responsive human sperm cells. *Biol. Reprod.* **68**, 2122-2134.

Demarco, I. A., Espinosa, F., Edwards, J., Sosnik, J., De La Vega-Beltran, J. L., Hockensmith, J. W., Kopf, G. S., Darszon, A. and Visconti, P. E. (2003). Involvement of a Na^+/HCO^{-3} cotransporter in mouse sperm capacitation. *J. Biol. Chem.* **278**, 7001-7009.

Escoffier, J., Boisseau, S., Serres, C., Chen, C. C., Kim, D., Stamboulian, S., Shin, H. S., Campbell, K. P., De Waard, M. and Arnoult, C. (2007). Expression, localization and functions in acrosome reaction and sperm motility of Ca(V)3.1 and Ca(V)3.2 channels in sperm cells: an evaluation from Ca(V)3.1 and Ca(V)3.2 deficient mice. *J. Cell Physiol.* **212**, 753-763.

Escoffier, J., Couvet, M., de Pomyers, H., Ray, P. F., Seve, M., Lambeau, G., De Waard, M. and Arnoult, C. (2010a). Snake venoms as a source of compounds modulating sperm physiology: Secreted phospholipases A2 from Oxyuranus scutellatus scutellatus impact sperm motility, acrosome reaction and in vitro fertilization in mice. *Biochimie* **92**, 826-836.

Escoffier, J., Jemel, I., Tanemoto, A., Taketomi, Y., Payre, C., Coatrieux, C., Sato, H., Yamamoto, K., Masuda, S., Pernet-Gallay, K. et al. (2010b). Group X phospholipase A2 is released during sperm acrosome reaction and controls fertility outcome in mice. *J. Clin. Invest.* **120**, 1415-1428.

Esposito, G., Jaiswal, B. S., Xie, F., Krajnc-Franken, M. A., Robben, T. J., Strik, A. M., Kuil, C., Philipsen, R. L., van Duin, M., Conti, M. et al. (2004). Mice deficient for soluble adenylyl cyclase are infertile because of a severe sperm-motility defect. *Proc. Natl. Acad. Sci. USA* **101**, 2993-2998.

Felix, R., Serrano, C. J., Trevino, C. L., Munoz-Garay, C., Bravo, A., Navarro, A., Pacheco, J., Tsutsumi, V. and Darszon, A. (2002). Identification of distinct K^+ channels in mouse spermatogenic cells and sperm. *Zygote* **10**, 183-188.

Flesch, F. M., Brouwers, J. F., Nievelstein, P. F., Verkleij, A. J., van Golde, L. M., Colenbrander, B. and Gadella, B. M. (2001). Bicarbonate stimulated phospholipid scrambling induces cholesterol redistribution and enables cholesterol depletion in the sperm plasma membrane. *J. Cell Sci.* **114**, 3543-3555.

Florman, H. M., Arnoult, C., Kazam, I. G., Li, C. and O'Toole, C. M. (1998). A perspective on the control of mammalian fertilization by egg-activated ion channels in sperm: a tale of two channels. *Biol. Reprod.* **59**, 12-16.

Fukami, K., Yoshida, M., Inoue, T., Kurokawa, M., Fissore, R. A., Yoshida, N., Mikoshiba, K. and Takenawa, T. (2003). Phospholipase Cdelta4 is required for Ca^{2+} mobilization essential for acrosome reaction in sperm. *J. Cell Biol.* **161**, 79-88.

Hernandez-Gonzalez, E. O., Sosnik, J., Edwards, J., Acevedo, J. J., Mendoza-Lujambio, I., Lopez-Gonzalez, I., Demarco, I., Wertheimer, E., Darszon, A. and Visconti, P. E. (2006). Sodium and epithelial sodium channels participate in the regulation of the capacitation-associated hyperpolarization in mouse sperm. *J. Biol. Chem.* **281**, 5623-5633.

Hernandez-Gonzalez, E. O., Trevino, C. L., Castellano, L. E., de la Vega-Beltran, J. L., Ocampo, A. Y., Wertheimer, E., Visconti, P. E. and Darszon, A. (2007). Involvement of cystic fibrosis transmembrane conductance regulator in mouse sperm capacitation. *J. Biol. Chem.* **282**, 24397-24406.

Hess, K. C., Jones, B. H., Marquez, B., Chen, Y., Ord, T. S., Kamenetsky, M., Miyamoto, C., Zippin, J. H., Kopf, G. S., Suarez, S. S. et al. (2005). The "soluble" adenylyl cyclase in sperm mediates multiple signaling events required for fertilization. *Dev. Cell* **9**, 249-259.

Johnson, L. A. (2000). Sexing mammalian sperm for production of offspring: the state-of-the-art. *Anim. Reprod Sci.* **60-61**, 93-107.

Konig, J., Schreiber, R., Voelcker, T., Mall, M. and Kunzelmann, K. (2001). The cystic fibrosis transmembrane conductance regulator (CFTR) inhibits ENaC through an increase in the intracellular Cl- concentration. *EMBO Rep.* **2**, 1047-1051.

Krapf, D., Arcelay, E., Wertheimer, E. V., Sanjay, A., Pilder, S. H., Salicioni, A. M. and Visconti, P. E. (2010). Inhibition of Ser/Thr phosphatases induces capacitation-associated signaling in the presence of Src kinase inhibitors. *J. Biol. Chem.* **285**, 7977-7985.

Lievano, A., Santi, C. M., Serrano, C. J., Trevino, C. L., Bellve, A. R., Hernandez-Cruz, A. and Darszon, A. (1996). T-type Ca^{2+} channels and alpha1E expression in spermatogenic cells, and their possible relevance to the sperm acrosome reaction. *FEBS Lett.* **388**, 150-154.

Lu, M., Dong, K., Egan, M. E., Giebisch, G. H., Boulpaep, E. L. and Hebert, S. C. (2010). Mouse cystic fibrosis transmembrane conductance regulator forms cAMP-PKA-regulated apical chloride channels in cortical collecting duct. *Proc. Natl. Acad. Sci. USA* **107**, 6082-6087.

Martinez-Lopez, P., Santi, C. M., Trevino, C. L., Ocampo-Gutierrez, A. Y., Acevedo, J. J., Alisio, A., Salkoff, L. B. and Darszon, A. (2009). Mouse sperm K^+ currents stimulated by pH and cAMP possibly coded by Slo3 channels. *Biochem. Biophys. Res. Commun* **381**, 204-209.

Martinez-Pastor, F., Mata-Campuzano, M., Alvarez-Rodriguez, M., Alvarez, M., Anel, L. and de Paz, P. (2010). Probes and techniques for sperm evaluation by flow cytometry. *Reprod. Domest. Anim.* **45 Suppl. 2**, 67-78.

McPartlin, L. A., Visconti, P. E. and Bedford-Guaus, S. J. (2011). Guanine-nucleotide exchange factors (RAPGEF3/RAPGEF4) induce sperm membrane depolarization and acrosomal exocytosis in capacitated stallion sperm. *Biol. Reprod.* **85**, 179-188.

Morgan, D. J., Weisenhaus, M., Shum, S., Su, T., Zheng, R., Zhang, C., Shokat, K. M., Hille, B., Babcock, D. F. and McKnight, G. S. (2008). Tissue-specific PKA inhibition using a chemical genetic approach and its application to studies on sperm capacitation. *Proc. Natl. Acad. Sci. USA* **105**, 20740-20745.

Munoz-Garay, C., De La, Vega-Beltran, J. L., Delgado, R., Labarca, P., Felix, R., and Darszon, A. (2001). Inwardly rectifying K(+) channels in spermatogenic cells: functional expression and implication in sperm capacitation. *Dev. Biol.* **234**, 261-274.

Nakanishi, T., Ikawa, M., Yamada, S., Parvinen, M., Baba, T., Nishimune, Y. and Okabe, M. (1999). Real-time observation of acrosomal dispersal from mouse sperm using GFP as a marker protein. *FEBS Lett.* **449**, 277-283.

Nakanishi, T., Ikawa, M., Yamada, S., Toshimori, K. and Okabe, M. (2001). Alkalinization of acrosome measured by GFP as a pH indicator and its relation to sperm capacitation. *Dev. Biol.* **237**, 222-231.

Piehler, E., Petrunkina, A. M., Ekhlasi-Hundrieser, M. and Topfer-Petersen, E. (2006). Dynamic quantification of the tyrosine phosphorylation of the sperm surface proteins during capacitation. *Cytometry A* **69**, 1062-1070.

Ren, D. and Xia, J. (2010). Calcium signaling through CatSper channels in mammalian fertilization. *Physiology (Bethesda)* **25**, 165-175.

Santi, C. M., Martinez-Lopez, P., de la Vega-Beltran, J. L., Butler, A., Alisio, A., Darszon, A. and Salkoff, L. (2010). The SLO3 sperm-specific potassium channel plays a vital role in male fertility. *FEBS Lett.* **584**, 1041-1046.

Schreiber, M., Wei, A., Yuan, A., Gaut, J., Saito, M. and Salkoff, L. (1998). Slo3, a novel pH-sensitive K^+ channel from mammalian spermatocytes. *J. Biol. Chem.* **273**, 3509-3516.

Schreiber, R., Hopf, A., Mall, M., Greger, R. and Kunzelmann, K. (1999). The first-nucleotide binding domain of the cystic-fibrosis transmembrane conductance regulator is important for inhibition of the epithelial Na+ channel. *Proc. Natl. Acad. Sci. USA* **96**, 5310-5315.

Tao, J., Critser, E. S. and Critser, J. K. (1993). Evaluation of mouse sperm acrosomal status and viability by flow cytometry. *Mol. Reprod Dev.* **36**, 183-194.

Tomes, C. N. (2007). Molecular mechanisms of membrane fusion during acrosomal exocytosis. *Soc. Reprod. Fertil.* **Suppl. 65**, 275-291.

Trevino, C. L., Serrano, C. J., Beltran, C., Felix, R. and Darszon, A. (2001). Identification of mouse trp homologs and lipid rafts from spermatogenic cells and sperm. *FEBS Lett.* **509**, 119-125.

Van Dilla, M. A., Gledhill, B. L., Lake, S., Dean, P. N., Gray, J. W., Kachel, V., Barlogie, B. and Gohde, W. (1977). Measurement of mammalian sperm deoxyribonucleic acid by flow cytometry. Problems and approaches. *J. Histochem. Cytochem.* **25**, 763-773.

Visconti, P. E. (2009). Understanding the molecular basis of sperm capacitation through kinase design. *Proc. Natl. Acad. Sci. USA* **106**, 667-668.

Visconti, P. E., Bailey, J. L., Moore, G. D., Pan, D., Olds-Clarke, P. and Kopf, G. S. (1995a). Capacitation of mouse spermatozoa. I. Correlation between the capacitation state and protein tyrosine phosphorylation. *Development* **121**, 1129-1137.

Visconti, P. E., Moore, G. D., Bailey, J. L., Leclerc, P., Connors, S. A., Pan, D., Olds-Clarke, P. and Kopf, G. S. (1995b). Capacitation of mouse spermatozoa. II. Protein tyrosine phosphorylation and capacitation are regulated by a cAMP-dependent pathway. *Development* **121**, 1139-1150.

Visconti, P. E., Galantino-Homer, H., Ning, X., Moore, G. D., Valenzuela, J. P., Jorgez, C. J., Alvarez, J. G. and Kopf, G. S. (1999a). Cholesterol efflux-mediated signal transduction in mammalian sperm. beta-cyclodextrins initiate transmembrane signaling leading to an increase in protein tyrosine phosphorylation and capacitation. *J. Biol. Chem.* **274**, 3235-3242.

Visconti, P. E., Ning, X., Fornes, M. W., Alvarez, J. G., Stein, P., Connors, S. A. and Kopf, G. S. (1999b). Cholesterol efflux-mediated signal transduction in mammalian sperm: cholesterol release signals an increase in protein tyrosine phosphorylation during mouse sperm capacitation. *Dev. Biol.* **214**, 429-443.

Wertheimer, E. V., Salicioni, A. M., Liu, W., Trevino, C. L., Chavez, J., Hernandez-Gonzalez, E. O., Darszon, A. and Visconti, P. E. (2008). Chloride Is essential for capacitation and for the capacitation-associated increase in tyrosine phosphorylation. *J. Biol. Chem.* **283**, 35539-35550.

Xu, W. M., Shi, Q. X., Chen, W. Y., Zhou, C. X., Ni, Y., Rowlands, D. K., Yi Liu, G., Zhu, H., Ma, Z. G, Wang, X. F. et al. (2007). Cystic fibrosis transmembrane conductance regulator is vital to sperm fertilizing capacity and male fertility. *Proc. Natl. Acad. Sci. USA* **104**, 9816-9821.

Yanagimachi, R. (1994). Fertility of mammalian spermatozoa: its development and relativity. *Zygote* **2**, 371-372.

Zeng, X. H., Yang, C., Kim, S. T., Lingle, C. J. and Xia, X. M. (2011). Deletion of the Slo3 gene abolishes alkalization-activated K+ current in mouse spermatozoa. *Proc. Natl. Acad. Sci. USA* **108**, 5879-5884.

Zeng, Y., Clark, E. N. and Florman, H. M. (1995). Sperm membrane potential: hyperpolarization during capacitation regulates zona pellucida-dependent acrosomal secretion. *Dev. Biol.* **171**, 554-563.

Zeng, Y., Oberdorf, J. A. and Florman, H. M. (1996). pH regulation in mouse sperm: identification of Na(+)-, Cl(-)-, and HCO3(-)-dependent and arylaminobenzoate-dependent regulatory mechanisms and characterization of their roles in sperm capacitation. *Dev. Biol.* **173**, 510-520.

Journal of Cell Science